

Color Marker Detection with Various Imaging Conditions and Occlusion for UAV Automatic Landing Control

Montika Sereewattana¹, Miti Ruchanurucks², Somying Thainimit³, Sakol Kongkaew⁴
Department of Electrical Engineer,
Kasetsart University, Bangkok, Thailand
g5514553400@ku.ac.th¹,
fengmtr@ku.ac.th², fengsy@ku.ac.th³,
g5417500321@ku.ac.th⁴

Supakorn Siddhichai
Image Processing Laboratory, National
Electronics and Computer Technology
Center, Pathumthani Thailand
supakorn.siddhichai@nectec.or.th

Shoichi Hasegawa
Precision and Intelligence Laboratory,
Tokyo Institute of Technology,
Yokohama, Japan, 226-8503
hase@pi.titech.ac.jp

Abstract—Detection of markers for fixed-wing unmanned aerial vehicles play a crucial role in finding a runway to land, automatically. This is because the vehicles cannot land in limited area like rotor-wing UAV. Landing with the fixed-wing need to have a runway that is long and has a lot of symbols for demonstrating the landing point or touch down point. On the other hand, markers are difficult to be searched for, owing to having uncontrollable variables: illumination conditions, diverse environment and object occlusion. Moreover, the number of symbols on runway is another challenging issue. The aircraft controlled by autopilot that is at a height of 100 meters, e.g., may not be able to capture the markers properly before landing. Thus, it cannot land suitably. In order to reduce the complexity of the runway, four circular color markers are utilized to be a simple set of markers for the runway. The number can be increased to 6, 8, etc. for runway length expansion. Our proposed procedure is then: After normalized RGB colors of runway images to alleviate illumination error, detecting markers by Hough circular transform can be searched for even with occlusion. Experimental result shows around 72 to 87 percent accuracy tested by capturing in different scenarios: several exposures, gradations of tone, lens flares, motion blurs and uniform noise as well as object occlusion.

Keywords—Marker Detection; Normalized RGB; Color Segmentation; Hough Transform; Automatic Landing

I. INTRODUCTION

Nowadays, unmanned aerial vehicles (UAVs) are highly prevalent in military and developing for aviation business. In these developments, one of the most interesting topics is automatic landing control in various environment and illumination conditions. The control is a high-risked issue, since it can cause damages to the aircraft, surrounding objects or people. Laiacker et al [1] used high performance sensors including GPS and IMU and vision-based approach in order to detect a runway at several weather conditions. Their algorithm also had the runway database, which consisted of the runway

outline and a landing trajectory. When the aircraft went close to the runway, the algorithm compared a database runway image with the camera image. Also use of bounding box before detecting runway was proposed. However, most research usually prefers to solve an automatic landing control with as little complexity as possible. Kong et al [2] gathered the research of vision-based autonomous landing system in last 20 years. The study collected both rotary-wing and fixed-wing UAVs works that used visual sensors for detecting runways. One remarkable point in this proposition was in outdoor environment for fixed-wing UAVs: the runway images were generally varied by illumination changes. Consequently, there were two methods to overcome different light variations: 1) color thresholding the differences between runway and surrounding environment and 2) infrared markers installed around the runway.

On the other hand, some research focused on lane detection instead. Borker et al [3] tried to locate lane marker at night with frustrated illumination. The steps firstly cropped the Region of Interest (ROI) from videos and then the videos were converted to gray-scale and blurred. After that edge-detection was performed. Finally, they used low resolution images for Hough transform, so that lane markers would be found and corrected by matched filter. However, the accuracy of [3] was not so impressive for lane detection at night because light reflection from artificial illumination reduced the contrast of lane marker. There are also works that focus on converting color domain. Sun et al [4] emphasized to convert the input image to HSI color space. [4] stated that the lane markers usually have higher saturation (S) and intensity (I) values than those of the street and less I value than that of the sky. Hence, lane marker segmentation was thresholded by adjusting Intensity-Saturation filter. Then connected component labeling was used to assure the location of the lane markers.

Moreover, under the complicated surroundings constraints, there are works like: Yuan et al [5] compared complexity of computation, sensitivity to noise and precision of detection between the Standard Hough Transform (SHT) and the Gradient Hough Transform (GHT) to discover circular markers in the image from unmanned rotor-craft. In summary, [5] showed that SHT could be more robust than GHT for detecting all circular markers at higher altitude. If combining 2 algorithms, GHT would help to correct the marker at low altitude. Gu and Xu [6] used robotic UAV (RUAV) in order to pick up a target object which is on a circular marker. Randomized Hough Transform (RHT) was selected to be a detecting algorithm, which chooses 3 points of a circle detected. The three values were used as a parameterized vector for defining the marker and decreasing the calculation complexity of HT. In addition, this paper applied Graphic Processing Unit (GPU) to detect the marker for speeding up the method. The experimental result of this suggested that the effectiveness of GPU calculation was superior to that of Central Processing Unit (CPU): the marking detection could be done in higher frame rates, faster processing time.

Furthermore, various markers' detection is also utilized in other fields of research such as digital image processing and biomedical system. In image processing, Zhang et al [7] presented a ball detection algorithm in complex background and illumination variation. The ball searching method started using Retinex, which is human perception-based algorithm, chromatically invariant in light changes. Adaptive HT was deemed suitable for finding a ball position. After that the image would be converted into two color space, HSV and Grayworld normalization (GN) described in [7]. Also, the result of this algorithm is 80.3 percent robust to different illuminations. In biomedical system, Sampe et al [8] applied a detection algorithm with gait system, which used markers to detect and track walk-motion. Different-color markers were mounted on the joints while walking. Videos were collected in various times and lighting conditions. HSI color model was chosen to convert videos and then the marker would be detected. The results of this paper indicated yellow-colored marker provides highest accuracy, being in diverse illuminations.

In this paper, the precision of circular color marker detection in different image conditions and with object occlusion is presented. Comparing to former works, we will further show which color of a circular marker is most suitable for plane-to-ground marker detection, on gray background. This would play a vital role when actual automatic landing is implemented. Comparison would be based mainly on HSV color domain and Hough Circle Transform. This paper is divided in following sections. Section II shows the image preparation procedures that enhance image and threshold markers before detecting. Section III describes a specific method of this work that detects all circular markers and returns their positions. In section IV, it shows experimental results. Finally, section V is conclusion and future work.

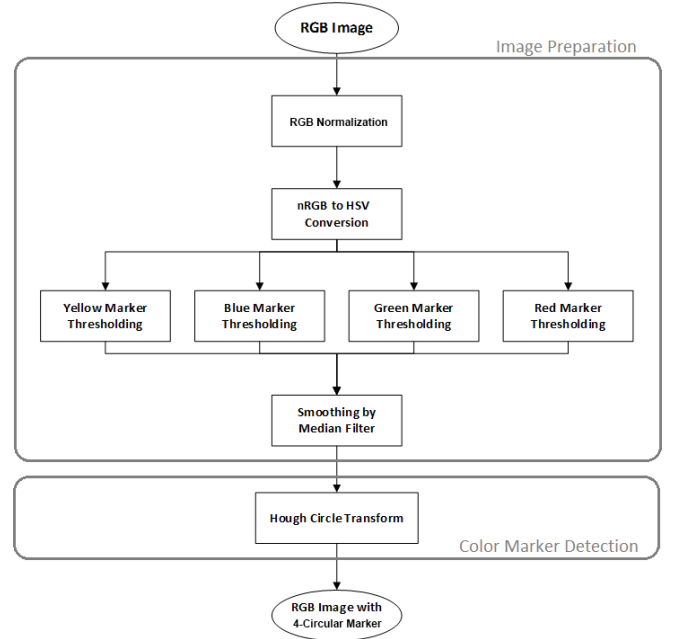


Fig. 1: Block diagram of color marker detection.

II. IMAGE PREPARATION

A. RGB Normalization ($nRGB$)

Normalizing RGB image is a process to alleviate intensity changes by dividing each color channel (R , G and B) of each pixel with summation of R , G and B .

$$nR = \frac{R}{R + G + B}, \quad nG = \frac{G}{R + G + B}, \quad nB = \frac{B}{R + G + B}$$

The new data are collected in percentage of its own channel. Denoting nR , nG and nB as the normalized colors of which summation is equal to one.

$$nR + nG + nB = 1$$

In our method, RGB images are converted to normalized RGB images as shown in Fig. 2. For reducing intensity in images before converting to HSV color space, the color information is clear from pixels that are in gray-scale.

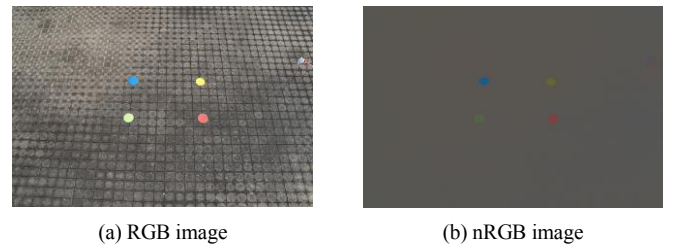


Fig. 2: Converting RGB to nRGB image

B. Converting nRGB image to HSV image

HSV or Hue-Saturation-Value is a color space that is represented in cylindrical coordinate. Hue (H) is the angle indicating the color around cylinder in the range of 0-359. Value (V) or brightness is the height of the cylinder taken in the range of 0-1. The third is saturation (S) which starts from the center of circle ($S = 0$) to the edge ($S = 1$). The HSV coordinate can be converted from RGB color space, provided that RGB values are normalized.

$$H = \arccos\left(\frac{R - \frac{1}{2}G - \frac{1}{2}B}{\sqrt{(R - G)^2 - (R - B)(G - B)}}\right)$$

$$S = \frac{\max(R, G, B) - \min(R, G, B)}{\max(R, G, B)}$$

$$V = \max(R, G, B)$$

In our method, calculation in HSV color space is preferred because illumination variation affects V and S whereas H remains quite stable in the range value.

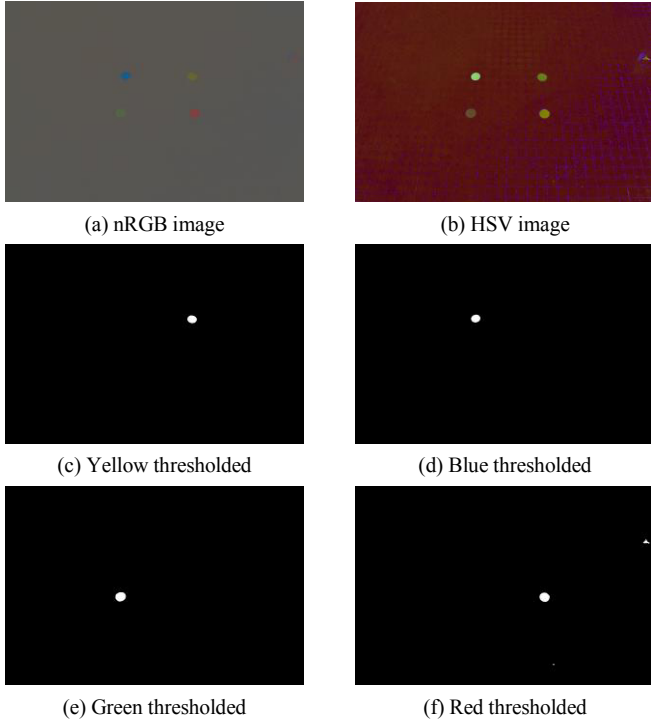


Fig. 3: Image preparation: image in 3(a) is in nRGB color space and 3(b) is in HSV color space, image in 3(c), 3(d), 3(e) and 3(f) are the examples of threshold and filtered images.

C. Color Marker Segmentation

After the image data are converted to HSV color space, segmentation of each color marker is an important procedure before detecting the circle. The suitable range of HSV of each marker was collected by picking up the hue, saturation and

value of each color in many lighting conditions. In this process of sampling the ranges from the data, threshold ranges of markers would be used in the system.

To make the images suitable for Hough Circle Transform, one image is converted to four binary images, each for a color marker. Finally, each marker image was filtered by median filter for eliminating outliers detected from the preceding step.

D. Median Filter

Median filter is usually applied for noise reduction. In order to decrease unwanted information, the filter runs through the image in each pixel and sorts the intensity of each pixel and its neighboring pixels using an $n \times n$ window. Then, the middle value is replaced to the pixel point. The remarkable advantage of median filter is that it can remove noise and preserve edges as well.

III. CIRCULAR MARKER DETECTION

After preparing the image data, there are four binary images which were thresholded by different criteria based on each marker's color, as shown in Fig. 3. The binary images are processed to detect special features of circular marker, from which Hough transform was selected to improve this algorithm.

A. Hough Circle Transform

Hough circle transform is generally used to detect the information of characters of a circle that is $(x - a)^2 + (y - b)^2 = r^2$ in which a and b are the circular center and r is the circular radius. In our research, the transform is used to find the circular forms of each marker in binary images which were extracted from a color image.

IV. EXPERIMENTAL RESULTS

A Sony ILCE QX-1 camera, 20 megapixels, is used for capturing images of four colored circular markers, with many illumination variations, on a fixed background of gray floor. The camera was set about 6 meters away from the runway mocking. Four markers were colored each by yellow, blue, green and red colors because the first one is usually applied for lane or runway marker and the others are primary color. Furthermore, another reason which the colors were chosen is almost all other markers on lane and runway are generally white color. Moreover, white can cause glare or reflection in images.

Among the illumination conditions, there are normal light, dim light, glare, and capturing with high and low exposure. On the other hand, some conditions are synthetically applied, namely gradient (gradation of tone), noise (in this paper: uniform), motion blur and lens flare. One extra condition is an object occlusion on marker. In the occlusion case, the above

mentioned illumination condition variations and synthetic conditions were further added for proving the robustness of this algorithm. All the conditions are shown in Fig. 4, where the markers in images are circled by Hough transform.

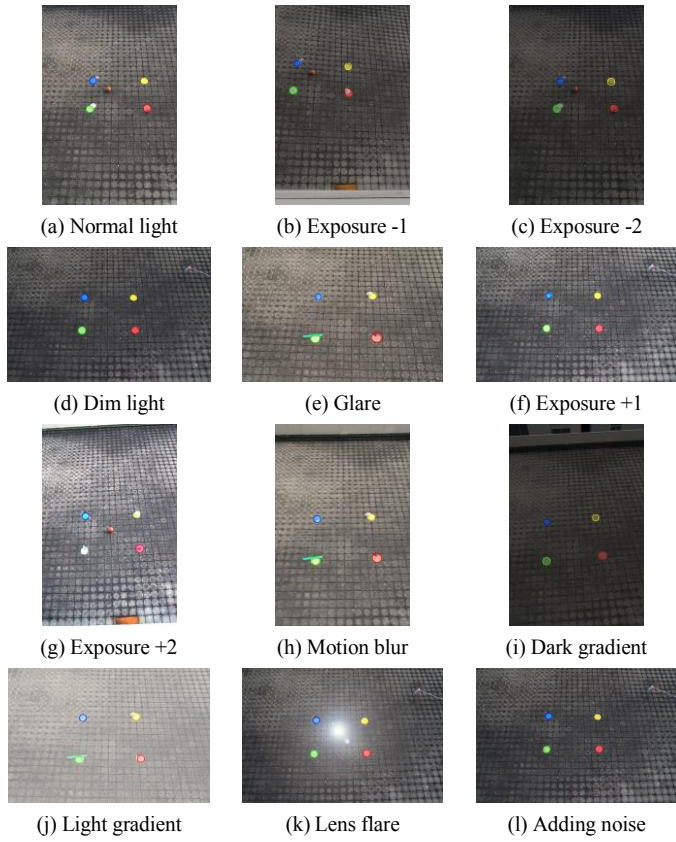


Fig. 4: All of the conditions which were applied for this algorithm.

In this experiment, 300 images, are used to be inputs for challenging the algorithm ability. In most case, the markers can be detected well by our method. Key ingredients are among the mentioned RGB normalization, HSV color space, Median filter, and Hough transform. For the results, in the Table I, blue-colored marker shows the highest accuracy of 87 percent. In some sense, the finding indicates that blue color is able to withstand noise and light changing. On the contrary, yellow, green and red are extremely affected from glares, high-level exposures, lens flares and noise; the detection errors, as shown in Fig. 5. Moreover, in the object occlusion case shown in Fig. 6, the algorithm could be detected the markers if an obstacle did not conceal over 60 percent of marker area.

V. CONCLUSION AND FUTURE WORK

Color marker detection with varying illumination conditions and occlusion for UAV automatic landing control was studied. Detection accuracy, overall, is 72-87 percent, depending on the color, brightness, glare, lens flare, motion blur and of course noise, which all were tested in this study, to

some certain extent. Essentially, up to our utmost knowledge, based on Sony lens and image sensor of model ILCE QX-1:

1. Blue-color marker yields the best detection result in all situations especially in high exposure or noise.
2. Red-color marker is especially affected by lens flare, which may be due to the fact that the artificial flare also contains many red pixels. (We also used other common flares, namely, white, red with blue, though.)
3. Object occlusion on circular marker must not cover the marker higher than 60 percent of its size.

Future work aims for applying these findings to localize a UAV without having to use GPS information by stereo vision and homography with a single camera and an orientation sensor.

TABLE I. COLOR MARKER DETECTION RESULTS

| Imaging Conditions | | | Detected Markers | | | |
|-------------------------------|--------|----|------------------|------|-------|-----|
| No or with occlusion (#image) | | | Yellow | Blue | Green | Red |
| Normal light | No occ | 3 | 3 | 3 | 3 | 3 |
| | Occ | 13 | 12 | 10 | 12 | 13 |
| Dim light | No occ | 3 | 3 | 3 | 3 | 3 |
| | Occ | 2 | 0 | 2 | 2 | 2 |
| Glare | No occ | 4 | 4 | 4 | 4 | 4 |
| | Occ | 5 | 2 | 4 | 4 | 5 |
| High exposure | No occ | 20 | 10 | 20 | 2 | 9 |
| | Occ | 40 | 16 | 35 | 5 | 17 |
| Low exposure | No occ | 20 | 20 | 20 | 20 | 20 |
| | Occ | 40 | 29 | 32 | 36 | 39 |
| Dark gradient | No occ | 10 | 10 | 10 | 10 | 10 |
| | Occ | 20 | 15 | 16 | 19 | 17 |
| Light gradient | No occ | 10 | 10 | 10 | 10 | 10 |
| | Occ | 20 | 18 | 17 | 16 | 18 |
| Lens flare | No occ | 10 | 9 | 9 | 10 | 6 |
| | Occ | 20 | 16 | 15 | 17 | 7 |
| Motion blur | No occ | 10 | 10 | 10 | 10 | 10 |
| | Occ | 20 | 19 | 16 | 18 | 20 |
| Adding noise | No occ | 10 | 0 | 10 | 2 | 6 |
| | Occ | 20 | 17 | 15 | 13 | 6 |
| Number of detected marker | | | 223 | 261 | 216 | 225 |
| Accuracy (percent) | | | 74.333 | 87 | 72 | 75 |

ACKNOWLEDGMENT

The authors would like to thank Thailand Advanced Institute of Science and Technology (TAIST) for scholarship, National Science and Technology Development Agency (NSTDA), Tokyo Institute of Technology and Kasetsart University (KU) under the TAIST Tokyo Tech

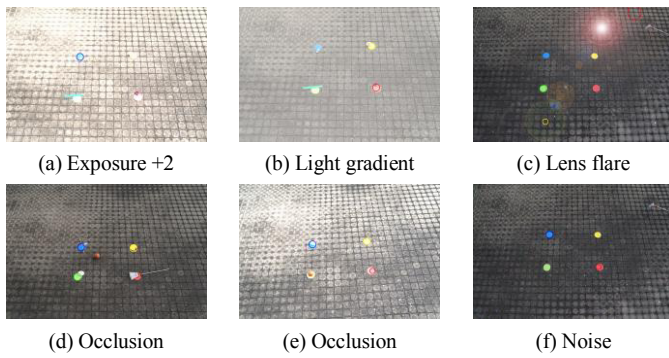


Fig. 5: Error of marker detection: image in 5(a), 5(b) and 5(c) are affected from illumination variations, image in 5(d) and 5(e) show detection error due to occlusion over 60 percent of marker area and image in 5(f) yellow and green markers cannot be detected because of noise is added to markers.

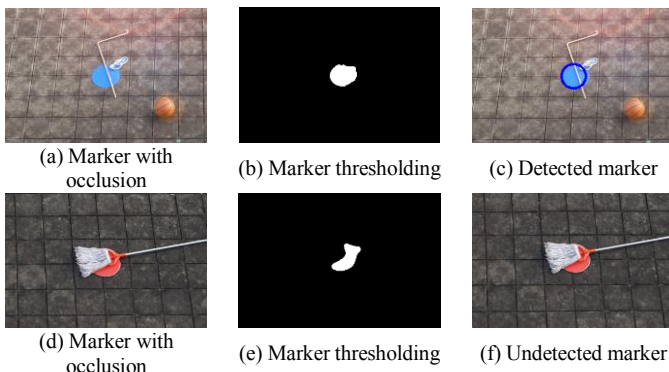


Fig. 6: Marker detection in the object occlusion case: image in 6(a), 6(b) and 6(c) show the procedure that can detect a color marker covered by object but image in 6(d), 6(e) and 6(f) cannot detect the marker because concealed over 60 percent by occlusion.

REFERENCES

- [1] M. Laiacker, K. Kondak, M. Schwarzbach, and T. Muskardin, "Vision aided automatic landing system for fixed wing uav," in *Intelligent Robots and Systems (IROS)*, 2013 IEEE/RSJ International Conference on, Nov 2013, pp. 2971–2976.
- [2] W. Kong, D. Zhou, D. Zhang, and J. Zhang, "Vision-based autonomous landing system for unmanned aerial vehicle: A survey."
- [3] A. Borkar, M. Hayes, M. Smith, and S. Pankanti, "A layered approach to robust lane detection at night," in *Computational Intelligence in Vehicles and Vehicular Systems*, 2009. CIVVS '09. IEEE Workshop on, March 2009, pp. 51–57.
- [4] T.-Y. Sun, S.-J. Tsai, and V. Chan, "Hsi color model based lane-marking detection," in *Intelligent Transportation Systems Conference*, 2006. ITSC '06. IEEE, Sept 2006, pp. 1168–1172.
- [5] M. Yuan, P. Feng, S. Haijun, L. Weixing, and G. Qi, "A method for unmanned rotorcraft to detect circular markers," in *Control Conference (CCC)*, 2014 33rd Chinese, July 2014, pp. 4758–4762.
- [6] A. Gu and J. Xu, "Vision based ground marker fast detection for small robotic uav," in *Software Engineering and Service Science (ICSESS)*, 2014 5th IEEE International Conference on, June 2014, pp. 975–978.
- [7] H. Zhang, Y. Wu, and F. Yang, "Ball detection based on color information and hough transform," in *Artificial Intelligence and Computational Intelligence*, 2009. AICI '09. International Conference on, vol. 2, Nov 2009, pp. 393–397.
- [8] I. Sampe, N. Amar Vijai, R. Tati Latifah, and T. Apriantono, "A study on the effects of lightning and marker color variation to marker detection and tracking accuracy in gait analysis system," in *Instrumentation, Communications, Information Technology, and Biomedical Engineering (ICICI-BME)*, 2009 International Conference on, Nov 2009, pp. 1–5.